ELSEVIER

Nuclear Physics A 677 (2000) 25–37

NUCLEAR PHYSICS A

www.elsevier.nl/locate/npe

Study of quadrupole moments of superdeformed bands in ^{145}Gd

T. Rząca-Urban [a], A. Pasternak [a,b], R.M. Lieder [c], W. Urban [a], M. Rejmund [a], Z. Marcinkowska [a], R. Marcinkowski [a], S. Utzelman [c], H.J. Jensen [c], W. Gast [c], H. Jäger [c], D. Bazzacco [d], S. Lunardi [d], N.H. Medina [d], R. Menegazzo [d], P. Pavan [d], C.M. Petrache [d], C. Rossi Alvarez [d], G. de Angelis [e], D.R. Napoli [e], L. Zhu [e], A. Dewald [f], S. Kasemann [f]

[a] *Institute of Experimental Physics, Warsaw University, ul. Hoża 69, PL-00-681 Warszawa, Poland*
[b] *A.F. Ioffe Physical Technical Institute RAS, RU-194021 St. Petersbourg, Russia*
[c] *Institut für Kernphysik, Forschungszentrum Jülich, D-52425 Jülich, Germany*
[d] *Dipartimento di Fisica dell'Università and Istituto Nazionale di Fisica Nucleare, Sezione di Padova, I-35131 Padova, Italy*
[e] *Istituto Nazionale di Fisica Nucleare, Laboratori Nazionali di Legnaro, I-35020 Legnaro, Italy*
[f] *Institut für Kernphysik, Universität zu Köln, D-50937 Köln, Germany*

Received 24 December 1999; revised 10 February 2000; accepted 25 April 2000

Abstract

Mean lifetimes have been measured for superdeformed bands of ^{145}Gd with the Doppler-shift attenuation method. The extracted quadrupole moments of the yrast and first excited superdeformed bands are $Q_0 = 11.8 \pm 0.8$ eb and $Q_0 = 13.2 \pm 1.0$ eb, respectively. The configuration assignments based on the quadrupole moments are $\pi 6^1 \pi[404]9/2 \nu[514]9/2 \nu 7^0$ for the yrast superdeformed band and $\pi 6^2 \nu[642]5/2 \nu 7^0$ for the first excited superdeformed band between the two known crossings.

PACS: 21.60.Cs; 23.20.Lv; 27.60.+j
Keywords: NUCLEAR REACTIONS: ^{114}Cd(^{36}S, 5n); $E = 182$ MeV; measured E_γ, I_γ; Doppler-shift attenuation; $\gamma\gamma\gamma$-coin; ^{145}Gd deduced superdeformed bands quadrupole moments, sidefeeding times, configurations; Compton-suppressed Ge-detector array

1. Introduction

Superdeformed (SD) bands have been well established in many nuclei in the mass 150 region. It was shown that the observed behaviour of the dynamic moment of inertia $\mathcal{J}^{(2)}$ as function of the rotational frequency depends sensitively on the number of occupied high-N

0375-9474/00/$ – see front matter
PII: S0375-9474(00)00223-2

intruder orbitals. In the nuclei of this mass region, the intruder orbitals are the $N = 6$ and $N = 7$ proton and neutron states originating from the $i_{13/2}$ and $j_{15/2}$ subshells. Therefore, the SD bands can be associated with $\pi 6^p \nu 6^{n_1} 7^{n_2}$ configurations where p, n_1 and n_2 are the number of occupied proton and neutron intruder orbitals. The large dynamic moment of inertia of a SD band is indicative of an elongated shape, but since the dynamic moment of inertia is also sensitive to other phenomena (like pairing and alignment effects) a more reliable measure of the deformation is the quadrupole moment of the SD band, as obtained in lifetime measurements. Since the quadrupole moment depends sensitively on the specific orbitals which are occupied, it becomes an important quantity to determine the configuration of a SD band. It was demonstrated in the cranking Skyrme–Hartree–Fock model [1] that, independently of intrinsic configurations and proton and neutron numbers, the quadrupole moment of a SD nucleus in the $A \approx 150$ region can be calculated very precisely with respect to the doubly-magic SD core nucleus ^{152}Dy in terms of the contributions of the individual hole and particle orbitals. The influence of the intruder orbitals on the quadrupole moment could only be probed recently as high-precision data obtained with large γ-ray spectrometer arrays became available. The dependence of the quadrupole deformation on the number of high-N intruder orbitals is well established in the $A \approx 150$ region from lifetime measurements for the SD bands of ^{148,149}Gd, ^{152}Tb [2], ^{151,152}Dy and ^{151}Tb [3]. A recent detailed theoretical investigation of polarization effects [4] showed that quadrupole moments of nuclei with even up to 10 particles removed from the SD core nucleus ^{152}Dy can be well described by simply subtracting effective quadrupole moments of the active single particle states from the quadrupole moment of the core.

In this report we present mean lifetime measurements for SD bands in ^{145}Gd. In our previous experiment [5] three SD bands have been found in this nucleus. The yrast SD band shows a smoothly decreasing dynamic moment of inertia with increasing rotational frequency. In the framework of the cranked Woods–Saxon–Strutinsky approach we assigned a $\pi 6^2 \nu 7^1$ configuration to this band. The first excited SD band shows two subsequent band crossings at rotational frequencies of ≈ 0.4 and 0.68 MeV, which were assigned to the subsequent alignments of an $i_{13/2}$ proton pair and a crossing of the $i_{13/2}[642]5/2$ and $i_{11/2}[651]1/2$ neutron orbitals, respectively. The $\nu 7_1$ orbital is not occupied. These features can be well reproduced by cranked Woods–Saxon–Strutinsky calculations provided that the yrast SD band has a larger deformation than the first excited SD band because the [770]1/2 neutron orbital gives a larger increase of the quadrupole deformation than the [642]5/2 and [651]1/2 orbitals [4]. More recently cranked relativistic mean field (CRMF) calculations [6] have been performed for a systematic study of all known yrast and in some cases also excited SD bands in the $A \approx 140-150$ region. According to these calculations for the yrast SD band in ^{145}Gd the 81st neutron is located in the [642]5/2 orbital at low rotational frequencies. At higher rotational frequencies, the character of this orbital changes to [651]1/2 due to a crossing which takes place at $\omega \approx 0.40$ MeV. This configuration does not contain any neutron in the $N = 7$ orbitals resulting in a $\nu 7^0$ configuration. This assignment differs from that proposed in our previous work [5] which suggested that the yrast band contains one $N = 7$ neutron. By measuring the lifetimes of SD bands in ^{145}Gd one can establish more conclusively which orbitals are active in the configurations of the SD bands.

2. Experimental details

High-spin states in ^{145}Gd have been populated in the ^{114}Cd(^{36}S, 5n) reaction at a beam energy of 182 MeV. The beam was provided by the XTU Tandem accelerator of the Legnaro National Laboratories. The target consisted of a 1.2 mg/cm^2 ^{114}Cd foil (enrichment 99.19%) evaporated on a multilayer backing. The backing consisted of Ta, Bi and Cu layers with thickness of 1.2 mg/cm^2 and 55 mg/cm^2 for Ta and Bi, respectively. The tantalum layer was added to prevent migration of the cadmium atoms into the bismuth backing due to target heating caused by the beam. The beam was stopped in the Bi layer and the Cu backing served to cool the target. The recoil velocity was $v/c = 2.5\%$. The γ-rays were detected using the GASP array which consists of 40 bismuth–germanate (BGO) suppressed Ge detectors and a 80 element BGO ball. Coincidence events were accepted only when the number of responding Compton-suppressed Ge detectors was greater than two and the BGO fold greater than eight. Under these conditions, a total of 1×10^9 events were collected on magnetic tapes. The Ge detectors in the GASP array are placed symmetrically with respect to the beam direction in seven rings, as follows: six at $\approx 35°$, six at $\approx 60°$, four at 72°, eight at 90°, four at 108°, six at $\approx 120°$ and six at $\approx 145°$.

The low-lying oblate states in ^{145}Gd have lifetimes larger than a few ps and thus the corresponding γ-transitions showed no Doppler shift and provided a reliable energy calibration for all detectors. In the off-line analysis the high-spin states of ^{145}Gd (including SD states) were enhanced by setting proper conditions on the inner BGO ball requiring a fold $\geqslant 15$. The lifetimes of the SD states in the $A \approx 150$ region are considerably shorter than the slowing down times of the recoiling nuclei, being typically a few ps. Therefore, most of the SD transitions are emitted from the recoiling nuclei with essentially the maximum Doppler shift. In the present experiment the Doppler shifts of transitions originating from states at the bottom of the SD bands were $\approx 70\%$ of the maximum shift. The analysis of the data is greatly simplified by this fact, since, if a correction with the maximum Doppler shift is applied, the majority of the SD peaks will be correctly gain-matched. Seven γ–γ–γ cubes have been produced, using the software package Ana [7]. Energies from any detector were sorted after full Doppler-shift correction into the first two axes and the uncorrected energies from detectors placed in one of the seven rings, available in the GASP geometry, were sorted into the third axis of the respective cubes. From these cubes coincidence spectra were obtained by double gating on SD band transitions in the first two axes and by projecting onto the third axis. Two of the spectra resulting for the yrast SD band in ^{145}Gd are presented in Fig. 1.

3. Analysis and results

In order to extract the lifetime information from the spectra obtained for the SD bands in ^{145}Gd the fraction of the full Doppler shift $F(\tau) = v/v_0$ has been determined for each transition. In the standard procedure, $F(\tau)$ is determined from the centroid E_c of a Doppler-shifted γ-line as measured at the angle Θ with respect to the beam direction according to:

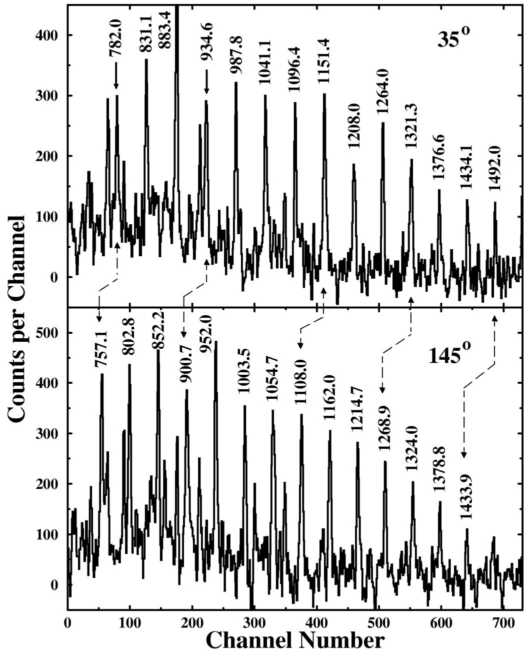

Fig. 1. Summed double-gated coincidence spectra corresponding to the detectors placed under angles of $\approx 35°$ and $\approx 145°$ with respect to the beam direction. The peaks belonging to the same transition are for a few cases connected by a dashed line.

$$E_c - E_0 = E_0 F(\tau)\frac{v_\circ}{c}x, \tag{1}$$

where E_0 is the unshifted γ-ray energy and $x = \cos(\Theta)$.

The experimental $F(\tau)$ values are compared with predictions obtained by taking into account the slowing-down process of the recoils and the deexcitation history for various values of the quadrupole moment Q_0 and the delay τ_{sf} due to sidefeeding.

The determination of the centroid is rather unreliable if the intensities of the SD transitions are fairly small, if transitions between low-spin states are superimposed or if tails due to Doppler effects cannot be distinguished from the background. In the present work the energies E_{top} of the maxima of the Doppler-shifted γ-lines, which can be determined reliably, have been used in the lifetime analysis. From lineshape calculations the centroids of the Doppler-shifted γ-lines have subsequently been evaluated. The difference between the maximum and the centroid of a γ-line can be parameterized in terms of a correction factor $K(x^2)$ as:

$$E_{\text{top}} - E_c = (E_c - E_0)K\left(x^2\right), \quad \text{where} \tag{2}$$

$$K\left(x^2\right) = \frac{a}{1 + \exp\left[-k\left(x^2 - x_c^2\right)\right]}. \tag{3}$$

The parameters a, k and x_c^2 depend on the quadrupole moment Q_0 and the sidefeeding delay τ_{sf}. For each set of Q_0 and τ_{sf} the values of these parameters have been determined from lineshape calculations taking into account the deexcitation history and the slowing-down process. From the energy differences $E_{\text{top}} - E_c$ the "experimental" $F(\tau)$ values are determined. Because of this procedure the $F(\tau)$ values are to some extent model dependent. Hence, the word experimental is set in quotation marks. However, the variation of $F(\tau)$ is smaller than its experimental uncertainty for values of the quadrupole moment ranging from 8 to 14 eb.

The detailed slowing-down histories of the recoiling nuclei, considering the effects of particle emission and target-backing composition on the velocity profile, has been calculated with a Monte Carlo procedure using the codes COMPA and GAMMA [8,9]. The recoil velocities were calculated with the code COMPA using a statistical model of the nuclear reaction. The slowing down of the recoils in the target and backing including multiple scattering was simulated with the code GAMMA. In these calculations it has been considered that the target and backing consisted of three materials, viz. Cd, Ta and Bi. The mean initial velocity of the recoils in Cd was $v_0/c = 0.025$ and the range of recoil velocities in the Ta and Bi layers were $v/c = 0.020 - 0.024$ and < 0.020, respectively. Practically all γ-rays from SD states with short effective lifetimes, belonging to the upper portion of the SD band, were emitted in the Cd and Ta layers. For the lower portion of the SD band the effective lifetime increases to > 100 fs and the stopping in Bi has to be taken into account as well.

The electronic and nuclear stopping powers have been calculated in the framework of the theory of Lindhard et al. (see Appendix of Ref. [10]). We used correction factors of $f_e = 1.22$, 1.12 and 1.17 for the electronic stopping powers of the Gd recoils in Cd, Ta and Bi, respectively. These correction factors are supported by experimental investigations of the electronic stopping power for heavy ions [11–14] in the range of velocities occurring in the present experiment ($v/c \leqslant 0.025$). For the nuclear stopping power we used a correction factor of $f_n = 0.8$. We assume that the accuracy of our stopping power evaluation is $\approx 10\%$, resulting in contributions of $\approx 5\%$ to the uncertainties to the quadrupole moments.

To extract the quadrupole moments of SD bands from the experimental $F(\tau)$ values it is essential to take properly into consideration the delay due to sidefeeding τ_{sf}. The relative intensities of the transitions in the yrast and excited SD bands of ^{145}Gd [5] as function of spin show similar profiles as those of other SD bands in this mass region. About seven high-spin members of the SD bands in ^{145}Gd receive feeding so that the intensities of the corresponding transitions increase with decreasing spin. The following transitions have approximately a constant intensity (plateau region). The deexcitation of the SD bands occur over the last two transitions [5].

Usually the assumption is made that the sidefeeding into the high-lying SD states can be approximated by a single rotational cascade of a few transitions with the same dynamic moment of inertia $\mathcal{J}^{(2)}$ as that of the SD band and a quadrupole moment Q_{sf}. The investigation of quadrupole moments of SD bands in ^{151}Dy, ^{151}Tb and ^{152}Dy by Nisius et al. [3] shows that for SD bands of ^{151}Dy and ^{151}Tb the $F(\tau)$ values for high-lying SD states are close to unity. For the SD band in ^{152}Dy it was found, however, that the corresponding values are consistently below one. The latter observation has been explained by an initial delay of 24 fs [3]. An explanation for the origin of such a significant delay in the feeding of the high-spin members of the SD band in ^{152}Dy has not been given [3]. We have calculated the entry state distributions for the ^{122}Sn(^{34}S, 5n)^{151}Dy and ^{122}Sn(^{34}S, 4n)^{152}Dy reactions at a beam energy of 175 MeV used in the experiment of Nisius et al. [3] with the code COMPA. For ^{151}Dy the entry state distribution lies close to the high-spin members of the SD band so that they may be fed by one or two fast dipole transitions. However, for ^{152}Dy the entry state distribution is shifted considerably higher in spin and excitation energy. This result may explain the initial delay observed for ^{152}Dy. The absence of a significant delay in the feeding at the top of the SD band in ^{152}Dy populated in the ^{120}Sn(^{36}S, 4n) reaction at a beam energy of 170 MeV [2] may be due to a different entry state distribution. We have subsequently calculated the entry state distribution for the ^{114}Cd(^{36}S, 5n)^{145}Gd reaction at a beam energy of 182 MeV used in the present experiment. Since large differences in energies and spins between the entry states and the top of the SD bands have been found as well, a long-lived sidefeeding component may be expected. Therefore, the usual sidefeeding model assuming a quadrupole moment Q_{sf} but no initial delay may not apply in our case and we have used the approach described below.

To find an appropriate approach to handle the sidefeeding we have used two models describing extreme situations. In model (a) we have assumed a population of the high-lying SD states by one sidefeeding transition each with the same lifetime τ_{sf} for each initial state. In model (b) we have assumed a long cascade with the same lifetime for each member of this cascade populating the SD band at the top. This is equivalent to the assumption that $I_{\mathrm{sdb}} = 1$ for all SD states and leads to an initial delay τ_{sf} for the highest observed SD state. This model corresponds to model I proposed by Moore et al. [15]. Both models describe the SD band in terms of two fit parameters, viz. Q_0 and τ_{sf}, but the meaning of τ_{sf} is different. The real feeding pattern is between these two limits. In Fig. 2 the $F(\tau)$ values obtained for models (a) and (b) are plotted as function of τ_{sf} for the 1240 keV transition of the yrast SD band in ^{145}Gd. Furthermore, its “experimental” $F(\tau)$ value is indicated. The level deexcited by this transition is the lowest member of the SD band receiving sidefeeding. Hence, it is expected that the dependence of $F(\tau)$ on τ_{sf} is sensitive to the sidefeeding model used in the calculation for the 1240 keV transition. From Fig. 2 it is obvious, however, that for sidefeeding times up to ≈ 40 fs the $F(\tau)$ values are very similar independent of the model describing the sidefeeding population. In the following analysis we have used model (b). In Fig. 3 $F(\tau)$ values are plotted as function of τ_{sf} for the 868 keV transition of the yrast SD band in ^{145}Gd for various values of the quadrupole moment Q_0 of the SD band. One can see that $F(\tau)$ depends weakly on τ_{sf} but strongly on Q_0 for a low-lying transition of the SD band. In Fig. 4 $F(\tau)$ values are plotted as function of Q_0 for the high-lying 1409 keV transition of the yrast SD band in ^{145}Gd for various values of the sidefeeding time τ_{sf}. One can see that $F(\tau)$ depends weakly on Q_0 but strongly on τ_{sf} for a high-lying transition of the SD band. Hence, one can expect that both fitting parameters, viz. Q_0 and τ_{sf}, can be determined with a high reliability.

In the analysis of the spectra obtained for the yrast and first excited SD bands in ^{145}Gd at seven detector angles we determined the maxima E_{top} of the Doppler-shifted γ-lines belonging to these bands. From line shape calculations the centroids of these γ-lines, E_c, have subsequently been evaluated utilizing the methods described above. The line shape calculations have been carried out for all combinations of five values for the quadrupole

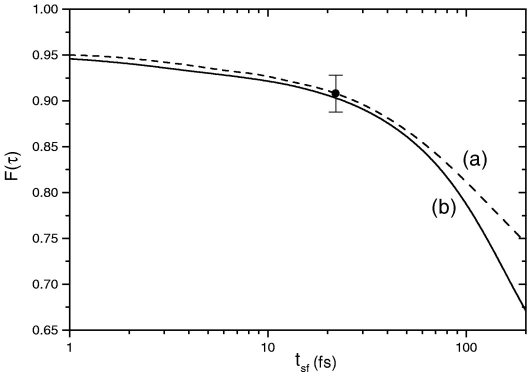

Fig. 2. Calculated fractional shifts $F(\tau)$ as function of the sidefeeding delay τ_{sf} for the 1240 keV transition of the yrast SD band in ^{145}Gd assuming (a) a sidefeeding of the upper portion of the SD band by one transition each and (b) a population of the SD band at the top by a long cascade. A quadrupole moment of $Q_0 = 11.8$ eb was assumed for the SD band.

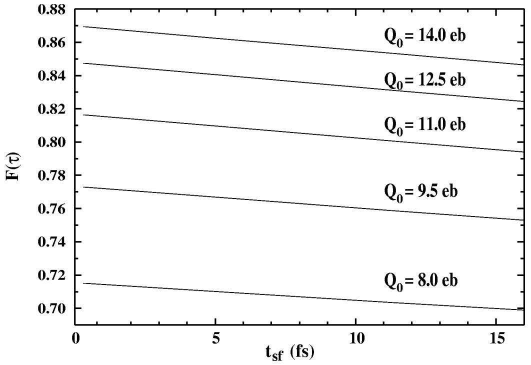

Fig. 3. Calculated fractional-shifts $F(\tau)$ as function of the sidefeeding delay τ_{sf} for the low-lying 868 keV transition of the yrast SD band in ^{145}Gd for various values of the quadrupole moment Q_0 of the SD band.

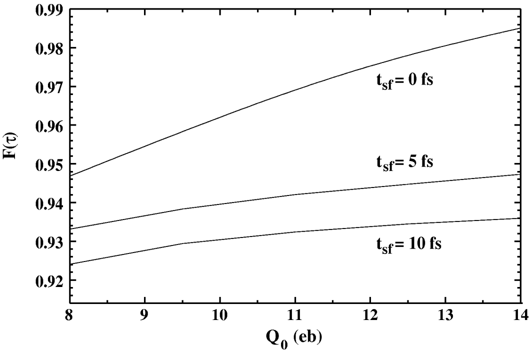

Fig. 4. Calculated fractional-shifts $F(\tau)$ as function of the quadrupole moment Q_0 for the high-lying 1409 keV transition of the yrast SD band in ^{145}Gd for various values of the sidefeeding delay τ_{sf}.

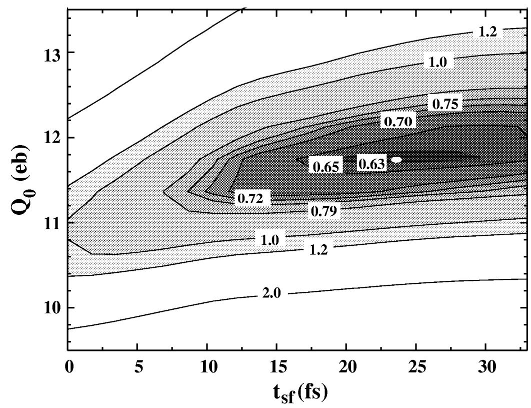

Fig. 5. Contour plot of χ^2 in a plane of the quadrupole moment Q_0 and the sidefeeding delay τ_{sf} for the yrast SD band in ^{145}Gd.

moment $Q_0 = 8.0$, 9.5, 11.0, 12.5 and 14.0 eb and six values for the sidefeeding delay $\tau_{sf} = 0.3$, 5.5, 11.3, 16.2, 23.4 and 33.6 fs. The line shapes have been calculated with the code SHAPE [8,9] for each SD transition, for each detector angle and for each value of the quadrupole moment and sidefeeding delay taking into account the slowing-down process. In the Monte Carlo calculation of the slowing-down process 300,000 events have been simulated. The results of this analysis are the "experimental" $F(\tau)$ values which have to be compared with the calculated $F(\tau)$ curves. Since the "experimental" $F(\tau)$ values depend on the quadrupole moments and sidefeeding delays a two-dimensional χ^2 minimization has been carried out to find the quadrupole moment and sidefeeding delay which reproduces best the experimental data. In Fig. 5 a χ^2 contour plot in a plane of the quadrupole moment Q_0 and the sidefeeding delay τ_{sf} is shown for the yrast SD band in ^{145}Gd. The contour plot shows a minimum for $Q_0 = 11.80 \pm 0.35$ eb and $\tau_{sf} = 23^{+12}_{-7}$ fs. The errors quoted here reflect only the statistical uncertainties in the determination of the γ-ray maxima E_{top}. To obtain the full error for the quadrupole moment of the yrast SD band, we included uncertainties of 5% for the stopping power parameters and 3% for the accuracy of the lineshape calculations, which gives $Q_0 = 11.8 \pm 0.8$ eb for the yrast SD band. For the quadrupole moment and the sidefeeding delay of the first excited SD band we obtained $Q_0 = 13.2 \pm 1.0$ eb and $\tau_{sf} = 16 \pm 5$ fs. In Fig. 6 $F(\tau)$ is plotted as function of γ-ray energy for the yrast and first excited SD bands. The "experimental" values of $F(\tau)$, as obtained for the quadrupole moments of 11.8 and 13.2 eb and sidefeeding delays of $\tau_{sf} = 23$ fs and 16 fs for the respective two SD bands are shown together with theoretical $F(\tau)$ curves for various values of the intrinsic quadrupole moments. Similar quadrupole moments have been found for the neighbouring nuclei ^{144,146}Gd [16,17].

4. Discussion

Many of the SD bands observed in $^{146-148}$Gd and the yrast SD band in ^{149}Gd are from investigations of the dynamic moments of inertia considered to have $\pi 6^2 \nu 7^1$ configurations

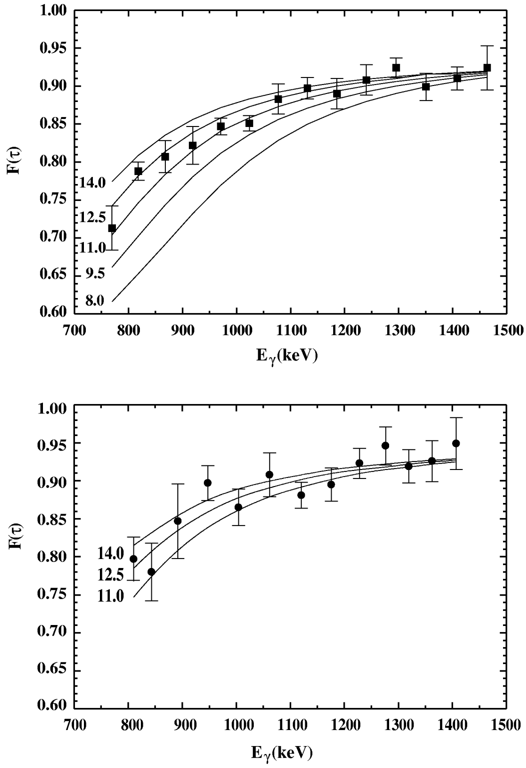

Fig. 6. "Experimental" fractional-shifts $F(\tau)$ as function of γ-ray energy and theoretical $F(\tau)$ curves for various values of the quadrupole moment Q_0 for the yrast SD band (upper portion) and the first excited SD band (lower portion) in ^{145}Gd. For more information see text.

(two protons in the $i_{13/2}$ orbital and one neutron in the $j_{15/2}$ orbital). Strong arguments for configuration assignments can be derived if band crossings are observed in SD bands. The crossing observed in the yrast SD band of ^{146}Gd is caused by the intersection of the $\nu i_{13/2}[642]5/2$ and $\nu i_{11/2}[651]1/2$ neutron orbitals [18]. Similar band crossings have been observed in SD bands of ^{147,148}Gd [20]. The yrast SD band found in ^{144}Gd [19] shows a sharp band crossing at a rotational frequency of $\hbar\omega$ = 0.45 MeV, which is interpreted as a crossing of the $\pi 6^0 \nu 7^0$ and $\pi 6^2 \nu 7^0$ configurations.

The yrast SD band in ^{145}Gd shows a smoothly decreasing dynamic moment of inertia with increasing rotational frequency. The first excited SD band shows two subsequent band crossings at rotational frequencies of ≈ 0.4 and 0.68 MeV. The second excited SD band shows no band crossing in the observed frequency range. In the framework of the cranked Woods–Saxon–Strutinsky approach the low-lying members of the SD bands in ^{145}Gd have been assigned to the $\pi 6^0 \nu[642]5/2 \nu 7^0$ and $\pi 6^0 \nu[514]9/2 \nu 7^0$ configurations [5]. At higher frequencies the $\pi 6^0 \nu[514]9/2 \nu 7^0$ configuration is crossed by the $\pi 6^2 \nu 7_1$ configuration. The alignment of the $i_{13/2}$ proton pair drives the nucleus to a larger deformation, and produces a pronounced rise in the dynamic moment of inertia $J^{(2)}$ at $\hbar\omega \approx 0.45$ MeV. In our previous paper [5] we assigned the $\pi 6^2 \nu 7^1$ configuration to the yrast SD band with a deformation of $\beta_2 = 0.523$. The $\pi 6^0 \nu[642]5/2 \nu 7^0$ configuration is crossed by a $\pi 6^2 \nu[642]5/2 \nu 7_0$ configuration which has been assigned to the first excited SD band in ^{145}Gd between the band crossings [5]. The first crossing observed in the latter band is due to the alignment of a pair of $N = 6$ protons and the second intersection is due to the crossing of the $\nu[642]5/2$ and $\nu[651]1/2$ orbitals. The calculated deformation for this band is $\beta_2 = 0.508$. The second excited SD band has been identified as the signature partner of the first excited SD band. This interpretation implies that both the yrast and first excited SD bands have a band crossing at $\hbar\omega \approx 0.40$ MeV. However, the increase of the dynamic moment of inertia is much larger for the first excited SD band than for the yrast SD band, an observation which has been explained by the different deformations.

The measured quadrupole moment of the yrast SD band in ^{145}Gd of $Q_0 = 11.8 \pm 0.8$ eb is smaller than that of the first excited SD band being $Q_0 = 13.2 \pm 1.0$ eb. The quadrupole deformation parameters β_2 have been deduced from the quadrupole moments as described in Ref. [21], taking into account hexadecapole deformations, resulting in $\beta_2 = 0.48$ for the yrast SD band and $\beta_2 = 0.52$ for the first excited SD band. The difference of the quadrupole moments is independent of the systematic uncertainties associated with the stopping powers. The measured quadrupole moments are in contradiction to the configuration assignments discussed above. Therefore, it is necessary to revise them. Already before our measurements it was proposed from CRMF calculations [6] that the configuration of the yrast SD band in ^{145}Gd does not contain a neutron in the $N = 7$ orbital.

In order to assign configurations to the SD bands in ^{145}Gd which are in agreement with the observed quadrupole moments the additivity rules for quadrupole moments in SD bands as proposed in [1,4] have been applied. To calculate the quadrupole moments for ^{145}Gd two protons and five neutrons have to be removed from the ^{152}Dy core. In order to reproduce the quadrupole moment of the yrast SD band we consider that the 81st neutron remains in the [514]9/2 orbital and that no crossing with the $N = 7$ intruder orbital occurs. The [514]9/2 orbital is less deformation driving than the $N = 7$ orbital. The [514]9/2 orbital probably crosses the 7_1 orbital at a higher frequency than suggested in our previous work [5]. Also the lack of a band crossing related to the occupation of the first $N = 7$ neutron orbital in the yrast SD band of ^{144}Gd at high frequencies [19] indicates that the $N = 7$ neutron orbital crosses the yrast SD band only at a larger rotational frequency. It is a clear indication that the 7_1 neutron intruder orbital is placed too low in energy if the Woods–Saxon potential is used. It is furthermore assumed that the 64th proton occupies the [404]9/2 instead of the $\pi 6_2$ orbital. This interpretation implies the absence of a crossing in the yrast SD band at $\hbar\omega \approx 0.40$ MeV, in agreement with the observation that the dynamic moment of inertia of this band does not show a pronounced increase at low rotational frequencies [5].

The measured quadrupole moment of the first excited SD band agrees fairly well with that calculated for the assigned configuration. Since furthermore the calculated moment of inertia reproduces fairly well the observed two band crossings [5] we suggest to keep the previous configuration assignment. Hence, our new configuration assignments are $\pi 6^1 \pi[404]9/2 \nu[514]9/2 \nu 7^0$ for the yrast SD band and $\pi 6^2 \nu[642]5/2 \nu 7^0$ for the first excited SD band between the two crossings.

The additivity rules have been applied to calculate the difference of the quadrupole moments of the yrast and first excited SD bands in ^{145}Gd. To reproduce the experimental difference between the quadrupole moments the 81st neutron has been placed in the [514]9/2 and [642]5/2 orbitals and the 64th proton in the [404]9/2 and $\pi 6_2$ orbitals, for the yrast and first excited SD bands, respectively. In Ref. [1] effective charge quadrupole moments q_2 have been extracted from Hartree–Fock mean-field calculations using a Skyrme force in the SkM* parameterization for most of the hole states necessary to calculate the quadrupole moments for the SD bands in ^{145}Gd with respect to the doubly-magic SD core nucleus ^{152}Dy utilizing the additivity rule. Only the effective quadrupole moment of the [660]1/2 proton hole configuration, required in our case, has not been reported in Ref. [1]. We have determined it using the HFODD (1.75) code [22], obtaining a value of $q_2 = -0.89$ eb. The calculated difference between the quadrupole moments of the two SD bands in ^{145}Gd is 1.61 eb in agreement with the measured difference of 1.4 ± 0.7 eb.

A quadrupole moment of $Q_0 = 13.7^{+1.1}_{-0.9}$ eb has been found in a recent experiment for the yrast SD band of ^{144}Gd above the band crossing [16]. This band has a $\pi 6^2 \nu 7^0$ configuration above the crossing deviating from that of the first excited SD band in ^{145}Gd between the two crossings only by a [642]5/2 neutron. The effective quadrupole moment for a neutron hole in this orbital is $q_2 = -0.22$ eb [1]. Therefore, it is expected that the quadrupole moment of the yrast SD band of ^{144}Gd is by 0.2 eb smaller than that of the first excited SD band in ^{145}Gd. Within statistical uncertainties the two experiments are in excellent agreement.

5. Summary

In conclusion, the quadrupole moments of two SD bands in ^{145}Gd have been measured using DSAM. The measured values of the quadrupole moments are $Q_0 = 11.8 \pm 0.8$ eb for the yrast SD band and $Q_0 = 13.2 \pm 1.0$ eb for the first excited SD band. The interpretation of these results requires a modification of the previous configuration assignment. Our results show that for the configuration assignment to the yrast SD band one should take into account the [404]9/2 proton configuration and consider that the [514]9/2 neutron orbital is not crossed by the neutron 7_1 intruder orbital because the latter is lying higher in excitation energy than expected from calculations using the Woods–Saxon potential. Our new configuration assignments are $\pi 6^1 \pi[404]9/2 \nu[514]9/2 \nu 7^0$ for the yrast SD band and $\pi 6^2 \nu[642]5/2 \nu 7^0$ for the first excited SD band between the two crossings.

Acknowledgements

We are indebted to the technical staff of the LNL for the careful operation of the XTU Tandem accelerator. We are very grateful to Jacek Dobaczewski for enlightening discussions and for making available the computer code HFODD. This work was supported by the Polish State Committee for Scientific Research (KBN) under grant 2P03B 05312 and by the Volkswagen Foundation under the contract number I/71976.

References

[1] W. Satuła, J. Dobaczewski, J. Dudek, W. Nazarewicz, Phys. Rev. Lett. 77 (1996) 5182.
[2] H. Savajols, A. Korichi, D. Ward, D. Appelbe, G.C. Ball, C. Beausang, F.A. Beck, T. Byrski, D. Curien, P. Dagnall, G. de France, D. Disdier, G. Duchêne, S. Erturk, C. Finck, S. Flibotte, B. Gall, A. Galindo-Uribarri, B. Hass, G. Hackman, V.P. Janzen, B. Kharraja, J.C. Lisle, J.C. Merdinger, S.M. Mullins, S. Pilotte, D. Prevost, D.C. Radford, V. Rauch, C. Rigollet, D. Smalley, M.B. Smith, O. Stezowski, J. Styczen, Ch. Theisen, P.J. Twin, J.P. Vivien, J.C. Waddington, K. Zuber, I. Ragnarsson, Phys. Rev. Lett. 76 (1996) 4480.
[3] D. Nisius, R.V.F. Janssens, E.F. Moore, P. Fallon, B. Crowell, T. Lauritsen, G. Hackman, I. Ahmed, H. Amro, S. Asztalos, M.P. Carpenter, P. Chowdhury, R.M. Clark, P.J. Daly, M.A. Deleplanque, R.M. Diamond, S.M. Fischer, Z.W. Grabowski, T.L. Khoo, I.Y. Lee, A.O. Macchiavelli, R.H. Mayer, F.S. Stephens, A.V. Afanasjev, I. Ragnarsson, Phys. Lett. B 392 (1997) 18.
[4] L.B. Karlsson, I. Ragnarsson, S. Åberg, Nucl. Phys. A 639 (1998) 654.
[5] T. Rząca-Urban, R.M. Lieder, S. Utzelmann, W. Gast, A. Georgiev, H.M. Jäger, D. Bazzacco, S. Lunardi, R. Menegazzo, C. Rossi Alvarez, G. de Angelis, D.R. Napoli, G. Vedovato, R. Wyss, Phys. Lett. B 356 (1995) 456.
[6] A.V. Afanasjev, J. König, P. Ring, Nucl. Phys. A 608 (1996) 107.
[7] W. Urban, in: Nuclear Physics Report 1991–1992, Manchester University, 1992, p. 95.
[8] A.E. Zobov, I.Kh. Lemberg, A.A. Pasternak, Izv. Akad. Nauk SSSR, Ser. Fiz. (Bull. Acad. Sci. USSR, Phys. Ser.) 54 (1990) 998.
[9] I.Kh. Lemberg, A.A. Pasternak, in: Modern Methods of Nuclear Spectroscopy, Nauka, Leningrad, 1985, p. 3.
[10] Ch. Briançon, V. Brudanin, J. Deutsch, V. Egorov, T. Filipova, M. Kudoyarov, V. Lobanov, T. Mamedov, A. Pasternak, R. Prieels, A. Salamatin, Yu. Shitov, Ts. Vylov, I. Yutlandov, Sh. Zaparov, accepted for publication in Nucl. Phys. A (1999).
[11] I.Kh. Lemberg, A.A. Pasternak, Nucl. Instrum. Methods 140 (1977) 71.
[12] K. Arstila, J. Keinonen, P. Tikkanen, Phys. Rev. B 41 (1990) 6117.
[13] K. Arstila, J. Keinonen, P. Tikkanen, Nucl. Instrum. Methods B 101 (1995) 321.
[14] F. Brandolini, N.H. Medina, M. De Poli, P. Pavan, M. Wilhelm, A. Dewald, G. Pascovici, Nucl. Inst. Meth. B 132 (1997) 11.
[15] E.F. Moore, D. Nisius, R.V.F. Janssens, T.L. Khoo, T. Lauritsen, D. Ackermann, I. Ahmad, H. Amro, D. Blumenthal, M.P. Carpenter, S. Fischer, G. Hackman, P. Fallon, S.J. Asztalos, R.M. Clark, M.A. Deleplanque, R.M. Diamond, R. Krücken, I.Y. Lee, A.O. Macchiavelli, F.S. Stephens, F. Hannachi, A. Lopez-Martens, J.A. Becker, L. Bernstein, L.P. Farris, E.A. Henry, A. Korichi, P. Chowdhury, R.H. Mayer, A.V. Afanasjev, I. Ragnarsson, in: Proc. Int. Conf. on Nuclear Structure at the Limits, Argonne, 1996, ANL/PHY-97/1, 1997, p. 72.
[16] C.A. Ur, D. Bazzacco, G.P. Bolzonella, S. Lunardi, N.H. Medina, C.M. Petrache, M.N. Rao, C. Rossi Alvarez, L.H. Zhu, G. de Angelis, A. De Acuna, D.R. Napoli, W. Gast, R.M. Lieder, T. Rząca-Urban, R. Wyss, Phys. Rev. C 60 (1999) 054302.
[17] A. Dewald, R. Krücken, P. Sala, J. Altmann, D. Weil, K.O. Zell, P. von Brentano, D. Bazzacco, C. Rossi Alvarez, R. Menegazzo, G. de Angelis, M. de Poli, in: The IV Int. Conf. Selected Topics in Nuclear Structure, Dubna, Russia, July 1994.
[18] G. Hebbinghaus, K. Strähle, T. Rząca-Urban, D. Balabanski, W. Gast, R.M. Lieder, H. Schnare, W. Urban, H. Wolters, E. Ott, J. Theuerkauf, K.O. Zell, J. Eberth, P. von Brentano, A. Alber,

K.H. Maier, W. Schmitz, E.M. Beck, H. Hübel, T. Bengtsson, I. Ragnarsson, S. Åberg, Phys. Lett. B 240 (1990) 311.
[19] S. Lunardi, L.H. Zhu, C.M. Petrache, D. Bazzacco, H. Medina, M.A. Rizzuto, C. Rossi Alvarez, G. de Angelis, G. Maron, D.R. Napoli, S. Utzelman, W. Gast, R.M. Lieder, A. Georgiev, F. Xu, R. Wyss, Nucl. Phys. A 618 (1997) 238.
[20] K. Zuber, D. Balouka, F.B. Beck, Th. Byrski, D. Curien, G. de France, G. Duchêne, G. Gehringer, B. Hass, J.C. Merdinger, P. Romain, D. Santos, J. Styczen, J.P. Vivien, J. Dudek, Z. Szymanski, T.R. Werner, Phys. Lett. B 254 (1991) 308.
[21] W. Nazarewicz, R. Wyss, A. Johnson, Nucl. Phys. A 503 (1989) 285.
[22] J. Dobaczewski, J. Dudek, Comp. Phys. Commun. 102 (1997) 166, 183 and to be published.